# Manuscript Details

| | |
|---|---|
| **Manuscript number** | AQTOX_2018_388_R1 |
| **Title** | Effects of nanosilver on Mytilus galloprovincialis hemocytes and early embryo development |
| **Article type** | Research Paper |


**Abstract**

Silver nanoparticles (AgNP), one of the main nanomaterials for production and use, are expected to reach the aquatic environment, representing a potential threat to aquatic organisms. In this study, the effects of bare AgNPs (47nm) on the marine mussel Mytilus galloprovincialis were evaluated at the cellular and whole organism level utilizing both immune cells (hemocytes) and developing embryos. The effects were compared with those of ionic Ag+ (AgNO3). In vitro short-term exposure (30 min) of hemocytes to AgNPs induced small lysosomal membrane destabilization (LMS EC50 = 273.1 µg/ml) and did not affect other immune parameters (phagocytosis and ROS production). Responses were little affected by hemolymph serum (HS) as exposure medium in comparison to ASW. However, AgNPs significantly affected mitochondrial membrane potential and actin cytoskeleton at lower concentrations. AgNO3 showed much higher toxicity, with an EC50 = 1.23 µg/ml for LMS, decreased phagocytosis and induced mitochondrial and cytoskeletal damage at similar concentrations. Both AgNPs and AgNO3 significantly affected Mytilus embryo development, with EC50 = 23.7 and 1 µg/L, respectively. AgNPs caused malformations and developmental delay, but no mortality, whereas AgNO3 mainly induced shell malformations followed by developmental arrest or death. Overall, the results indicate little toxicity of AgNPs compared with AgNO3; moreover, the mechanisms of action of AgNP appeared to be distinct from those of The results indicate little contribution of released Ag+ in our experimental conditions. These data provide a further insight into potential impact of AgNPs in marine invertebrates.


| | |
|---|---|
| **Keywords** | Nanosilver; Mytilus; hemocyte; immunity; mitochondria; cytoskeleton; embryos |
| **Taxonomy** | Aquatic Invertebrates, Early Embryonic Development, Nanoparticles, Bivalvia |
| **Corresponding Author** | Laura Canesi |
| **Corresponding Author's Institution** | Dept. of Eart, Environmental and Life Sciences, University of Genoa |
| **Order of Authors** | Manon Auguste, CATERINA CIACCI, teresa balbi, Andrea Brunelli, Valentina Caratto, Antonio Marcomini, Riccardo Cuppini, Laura Canesi |
| **Suggested reviewers** | Awadhesh Nandan Jha, Julian Blasco, M. Bebianno |

## Submission Files Included in this PDF

**File Name [File Type]**

CoverLettREV.docx [Cover Letter]

ResponseTorRviewers.docx [Response to Reviewers]

Highlights.docx [Highlights]

RevisedMS.docx [Manuscript File]

Fig1.tif [Figure]

Fig2.tif [Figure]

Fig3.tif [Figure]

Fig4.tif [Figure]

Fig5.tif [Figure]

Fig6.tif [Figure]

Fig7.tif [Figure]

To view all the submission files, including those not included in the PDF, click on the manuscript title on your EVISE Homepage, then click 'Download zip file'.

## Research Data Related to this Submission

There are no linked research data sets for this submission. The following reason is given:
Data will be made available on request

**Highlights**

- AgNPs do not affect immune parameters of *Mytilus* hemocytes in both ASW and HS
- AgNPs induced mitochondrial and cytoskeletal damage
- AgNPs decreased normal larval development and induced malformations in D-larvae
- AgNPs are much less toxic than $Ag^+$ in both mussel hemocytes and embryos
- The mechanisms of action of AgNPs appear to be distinct from those of $Ag^+$

# Effects of nanosilver on *Mytilus galloprovincialis* hemocytes and early embryo development

M. Auguste[1], C. Ciacci[2], T. Balbi[1], A. Brunelli[3], V. Caratto[4], A. Marcomini[5], R. Cuppini[2], L. Canesi[1]*

[1]*Dept. of Earth, Environment and Life Sciences (DISTAV), University of Genoa, Genoa, Italy.*

[2]*Dept. of Biomolecular Sciences (DIBS), University of Urbino, Italy*

[3]*Dept. of Geosciences, University of Vienna, Austria*

[4]*Dept. of Chemistry and Industrial Chemistry (DICCI), University of Genoa, Genoa, Italy.*

[5] *Dept. of Environmental Sciences, Informatics and Statistics (DAIS), Ca' Foscari University, Venice, Italy*

* Corresponding Author: laura.canesi@unige.it

**Key words**

*Nanosilver, Mytilus, hemocyte, immunity, mitochondria, cytoskeleton, embryos*

**Abstract**

Silver nanoparticles (AgNP), one of the main nanomaterials for production and use, are expected to reach the aquatic environment, representing a potential threat to aquatic organisms. In this study, the effects of bare AgNPs (47nm) on the marine mussel *Mytilus galloprovincialis* were evaluated at the cellular and whole organism level utilizing both immune cells (hemocytes) and developing embryos. The effects were compared with those of ionic $Ag^+$($AgNO_3$). In vitro short-term exposure (30 min) of hemocytes to AgNPs induced small lysosomal membrane destabilization (LMS $EC_{50}$ =273.1 µg/mL) and did not affect other immune parameters (phagocytosis and ROS production). Responses were little affected by hemolymph serum (HS) as exposure medium in comparison to ASW. However, AgNPs significantly affected mitochondrial membrane potential and actin cytoskeleton at lower concentrations. $AgNO_3$ showed much higher toxicity, with an $EC_{50}$ =1.23 µg/mL for LMS, decreased phagocytosis and induced mitochondrial and cytoskeletal damage at similar concentrations.

Both AgNPs and $AgNO_3$significantly affected *Mytilus* embryo development, with $EC_{50}$= 23.7 and 1 µg/L, respectively. AgNPs caused malformations and developmental delay, but no mortality, whereas $AgNO_3$ mainly induced shell malformations followed by developmental arrest or death.

Overall, the results indicate little toxicity of AgNPs compared with $AgNO_3$; moreover, the mechanisms of action of AgNP appeared to be distinct from those of $Ag^+$. The results indicate little contribution of released $Ag^+$ in our experimental conditions. These data provide a further insight into potential impact of AgNPs in marine invertebrates.

## 1. Introduction

Silver nanoparticles (AgNPs) have a large number of applications for their chemico-physical characteristics and, above all, in virtue of their biocidal action. The widespread utilization of AgNPs in a large range of consumer products, including textiles, care products and food packaging, will inevitably lead to their release in the environment (reviewed in Pulit-Prociak and Banach, 2016; McGillicuddy et al., 2017). According to Gottschalk et al. (2009) Predicted Environmental Concentrations (PECs) of AgNP for surface water in Europe are expected to be in the low ng/L-range (0.76ng/L), but it is expected to be released in larger quantities within the next decades (Fabrega et al., 2011; McGillicuddy et al., 2017). Once in the aquatic environment, AgNPs can undergo several transformation processes (agglomeration/aggregation, oxidation, dissolution, adsorption with soluble and particulate organic matter); in particular, release of $Ag^+$ ions may represent an additional source of silver in the environment (Levard et al., 2012; Sendra et al., 2017). With regards to ecotoxicity, it is widely acknowledged that the impact of AgNPs mainly depend on the $Ag^+$ released from the nanomaterial (Jemec et al., 2016).However, AgNPs may also exhibit a particle-specific toxicity, possibly mediated by physical interactions of the nanoparticulate form with biological systems(Li et al., 2014; Fabrega et al., 2011; Magesky and Pelletier 2018).

The impact of AgNPs has been widely investigated in marine invertebrates; these studies showed that *in vivo* exposure lead to silver accumulation, and different types of responses at molecular, cellular and tissue level (reviewed in Magesky and Pelletier 2018). The bivalve *Mytilus spp.* Is considered a suitable model for studying the effects and mechanisms of action of different types of NPs (Canesi et al., 2012; Canesi and Procházová 2013; Rocha et al., 2015; Canesi and Corsi, 2016; Beyer et al., 2017; Fagio et al., 2018). *In vivo* exposure to AgNPs have previously shown silver accumulation, induction of oxidative stress and damage to several cell components, including DNA (Zuykov et al., 2011; Gomes et al., 2013;McCarthy et al., 2013; Jimeno-Romero et al., 2017). These

data provided valuable information at the whole organism level, also considering different potential pathway of exposure.

With regards to *in vitro* data, the application of a battery of functional tests on *Mytilus* immune cells, the hemocytes, has been proven as a powerful tool for the rapid *in vitro* screening of the immunomodulatory effects and identification of the mechanisms of action of different types of NPs (Canesi et al., 2012; Canesi and Procházková, 2013; Canesi and Corsi, 2016; Canesi et al., 2016). These studies also underlined the importance of exposure medium in determining particle behaviour and interactions with target cells in a physiological environment (Balbi et al., 2017a, Canesi et al., 2017). However, information on the impact of AgNPs in bivalves at the cellular level is scarce, with only one study available to date. Exposure of *M. galloprovincialis* hemocytes and gill cells to several types of maltose-coated AgNPs of different sizes revealed higher toxicity of smaller size NPs, damages to cell components and activation of cellular defences after 24 h (Katsumiti et al., 2015). These data underlined the importance to further investigate the *in vitro* effects of AgNPs in mussel cells, in order to better understand their mechanism of action and possible toxicity.

In marine invertebrates, NPs generally do not have lethal effects at environmental concentrations, but can induce changes in their life cycle, growth or anatomical deformities, that can lead to a diminished biological performance of wild populations (Canesi and Corsi 2016). The application of developmental assays, involving exposure during the most sensitive stages of the organisms to environmental contaminants, would greatly help in the fast screening of NP toxicity (Fabbri et al., 2014). Most data are available on the sea urchin model, where exposure to nanoparticulate and ionic silver induced distinct effects depending on the life stage (Šiller et al., 2013; Magesky and Pelletier 2018). Developmental effects were also reported for AgNPs in oysters (Ringwood et al., 2010). However, no information is available on the effects of AgNPs on *Mytilus* embryos.

In the present study, the effects of bare AgNPs were investigated at the cellular level in short term *in vitro* experiments of *M. galloprovincialis* hemocytes; the impact on mussel early embryo

development was also evaluated. Parallel experiments were carried out using $AgNO_3$ in order to compare the effects of ionic silver. Hemocytes were exposed *in vitro* for 30 min to different concentrations of AgNPs (0.1-1000 µg/mL) or $AgNO_3$ (0.1-10 µg/mL) and Lysosomal Membrane Stability (LMS) was first evaluated as a marker of cellular stress. Functional immune parameters were also evaluated (extracellular reactive oxygen species-ROS production, phagocytosis). Experiments with AgNPs were carried out in either artificial sea water (ASW) or hemolymph serum (HS) to evaluate the influence of exposure medium. Moreover, at selected concentrations of AgNPs and $AgNO_3$, the effects on mitochondrial membrane potential and on actin cytoskeleton were evaluated by Confocal Laser Scanning Microscopy (CLSM).

The developmental effects of AgNPs were evaluated by the 48 h embryotoxicity test; fertilized eggs were exposed to AgNP (0.001-1000 µg/L) or $AgNO_3$ (0.1-25 µg/L). At the end of the assay, both percentage of normal D-larvae and the type of effect (malformations, delayed development, death) were evaluated.

## 2. Materials and methods

### *2.1. Characterization of NPs*

AgNPs (47MN-03) were purchased from Advanced Materials Inframat. The sample is a silver, black and ultrafine nanopowder with no coating. Characterization of primary particles and AgNP suspensions were performed as previously described (Brunelli et al., 2013). The average size of particle distribution of primary particles was evaluated by HR-TEM (High Resolution Transmission Microscopy) using a JEOL (Tokyo, Japan) 3010 microscope operating at 300 kV. Specific surface area was evaluated using BET method by nitrogen adsorption on a Micromeritics (Norcross, GA, USA) ASAP 2000 instrument, with an adsorption temperature of -196 °C, and pre-treating under high vacuum at 300 °C for 2 h.

Particle suspensions were prepared using 20 mg of AgNPs powder in 20 mL of Artificial Marine Water (AMW, ASTM D1141-98; pH7) and the suspension was sonicated for 15 min at 40 W, pulsed 10% using a probe sonication in an ice bath. The desired dilutions were made in AMW or mussel hemolymph serum (HS). Both suspensions (10; 50; 100 mg/L for AMW and 10 mg/L for HS) were characterized: hydrodynamic size distribution and agglomeration were determined by Dynamic Light Scattering (DLS) with a Nicomp Submicron Particle Sizer Autodilute® Model 370 (Santa Barbara, CA, USA), using a 90° scattering angle (Brunelli, 2013). ζ-potential values was measured using Electrophoretic light scattering.

For exposure experiments, AgNP was suspended in milliQ water at 1 mg/mL and homogenized using a probe sonication for 15 min in an ice bath. The next dilutions to obtain the desired exposure concentrations were made in either artificial seawater (ASW, pH 8) or hemolymph serum (HS), depending on the experiment. To obtain HS, the hemolymph was freshly extracted from mussels, filtered with gauze and centrifuged at 500 xg at 4°C for 10 min, and the supernatant was collected (Canesi et al., 2017). The different suspensions were in turn sonicated for 15 min prior to use. Stock solutions of silver nitrate ($AgNO_3$) were prepared in milliQ water at 1 mg/mL and diluted in ASW to obtain the desired exposure concentrations.

*2.2. Mussels and hemocyte sample preparations*

Mussels (*M. galloprovincialis* Lam.), were purchased in 2017 from an aquaculture farm in the Ligurian Sea (La Spezia, Italy) out of the main spawning period (February-March) for hemocyte functional assays. Mussels were transferred to the laboratory and acclimatized in static tanks containing aerated artificial sea water-ASW (ASTM, 2004), pH 7.9-8.1, 36 ppt salinity (1 L/animal), at 16 ± 1 °C. Hemolymph was extracted from the adductor muscle of 4-5 animals, using a syringe with an 18 G1/2'' needle, filtered with gauze, and pooled. Hemocyte monolayers were prepared as previously described (Canesi et al., 2010).

*2.3 Lysosomal membrane stability (LMS) and phagocytosis*

LMS was evaluated by the NRR (Neutral Red Retention time) assay as previously described (Ciacci et al., 2012; Canesi et al., 2010, 2015; Balbi et al., 2017b). Hemocyte monolayers on glass slides were incubated with 20 µL of the AgNP suspension in filtered ASW or HS for 30 min to reach the desired final concentrations of 0.1-0.5-1-5-10-50-100-500-1000 µg/mL. Parallel experiments were carried out with $AgNO_3$ at the final concentrations of 0.1-0.2-0.5-1-1.5-2-10 µg/mL in ASW. After incubation, the medium was removed and cells were incubated with a neutral red (NR) solution (final concentration 40 µg/mL from a stock solution of NR 40 mg/mL in DMSO); after 15 min excess dye was washed out and 20 µL of ASW was added. Every 15 min, slides were examined under an optical microscope and the percentage of cells showing loss of the dye from lysosomes in each field was evaluated. For each time point 10 fields were randomly observed, each containing 8–10 cells. The end point of the assay was defined as the time at which 50% of the cells showed sign of lysosomal leaking (the cytosol becoming red and the cells rounded). All incubations were carried out at 16 °C.

Phagocytic activity was evaluated as uptake of Neutral Red-conjugated zymosan particles in hemocyte monolayers as previously described (Ciacci et al., 2012). Hemocytes monolayers were incubated with AgNP and $AgnO_3$ for 30 min. Neutral Red-stained zymosan in 0.05 M Tris-HCl buffer (TBS), pH 7.6, containing 2.5% NaCl was added to each monolayer at a concentration of about 1:50 hemocytes:zymosan diluted in filtered ASW, and allowed to incubate for 60min at 16 °C. Monolayers were then washed three times with ASW, fixed with Baker's formol calcium (4% v/v formaldehyde, 2%NaCl, 1% calciumacetate) for 30 min and mounted in Kaiser's medium for microscopical examination with an inverted Olympus IX53 microscope (Olympus, Milano, Italy). For each slide, the percentage of phagocytic hemocytes was calculated from a minimum of 200 cells. Data are expressed as % of phagocytizing cells.

*2.4. Confocal Laser Scanning Microscopy (CLSM)*

Hemocytes were exposed to AgNPs (5, 10, 50 µg/mL in ASW) or $AgNO_3$ (0.2 and 1 µg/mL) for 30 min. Cells were fixed with paraformaldehyde at 4% for 10 min, washed two times for 2 min with TBS (0.05 M Tris-HCl buffer, pH 7.8) and permeabilized with 0.05% NP-40 (Nonidet-40) for 10 min.

Mitochondrial membrane potential (MMP, $\Delta\psi m$) was evaluated by the fluorescent dye Tetramethylrhodamine ethyl ester perchlorate (TMRE) as previously described (Ciacci et al., 2012; Canesi et al., 2008, 2015). TMRE is a quantitative marker for the maintenance of the mitochondrial membrane potential and it is accumulated within the mitochondrial matrix in accordance to the Nernst equation. TMRE exclusively stains the mitochondria and is not retained in cells upon collapse of the $\Delta\psi m$. Hemocytes were incubated with 40 nM TMRE for 10 min and observed by confocal microscopy.

Actin cytoskeleton structure was evaluated in hemocytes loaded with ActinGreen™488 ReadyProbes® Reagent for 30 min to reveal F-actin.

Fluorescence of TMRE (excitation 568 nm, emission 590-630 nm), and ActinGreen™488 (excitation 495 nm, emission 518 nm) was detected using a Leica TCS SP5 confocal setup mounted on a Leica DMI 6000 CS inverted microscope (Leica Microsystems, Heidelberg, Germany) using a 63x 1.4 oil objective (HCX PL APO 63.0-1.40 OIL UV). Images were analysed by the Leica Application Suite Advanced Fluorescence (LASAF) and ImageJ Software (Wayne Rasband, Bethesda, MA).

*2.5 Mussels and gamete collection*

Mussels sampled at the main spawning season (Feb-March) were transferred to the laboratory and acclimatized in static tanks containing aerated artificial sea water (ASTM, 2004), pH 7.9-8.1,

36 ppt salinity (1 L/animal), at 16 ± 1°C.Mussels were utilized within 2 days for gamete collection as previously described (Fabbri et al., 2014). When mussels beginning to spontaneously spawn were observed, each individual was immediately placed in a 250 mL beaker containing 200 mL of aerated ASW until complete gamete emission. After spawning, mussels were removed from beakers and sperms and eggs were sieved through 50 μm and 100 μm meshes, respectively, to remove impurities. Egg quality (shape, size) and sperm motility were checked using an inverted microscope. Eggs were fertilized with an egg:sperm ratio 1:10 in polystyrene 96-microwell plates (Costar, Corning Incorporate, NY, USA). After 30 min fertilization success (n. fertilized eggs / n. total eggs × 100) was verified by microscopical observation (>85%).

*2.6 Embryotoxicity test*

The 48-h embryotoxicity assay (ASTM, 2004) was carried out in 96-microwell plates according to Fabbri et al. (2014). Aliquots of 20 μL of 10x suspensions of AgNPs or of $AgNO_3$ solutions, suitably diluted in filter sterilized ASW, were added to fertilized eggs in each microwell to reach the nominal final concentrations (0-1000 μg/L for AgNPs and 0-25 μg/L for $AgNO_3$) in a 200 μL volume. Microplates were gently stirred for 1 min, and then incubated at 18 ± 1°C for 48 h, with a 16 h:8 h light:dark photoperiod. At the end of the incubation time, samples were fixed with buffered formalin (4%). A larva was considered normal when the shell was D-shaped (straight hinge) and the mantle did not protrude out of the shell, and malformed if had not reached the stage typical for 48 h (trocophora or earlier stages) or when some developmental defects were observed (concave, malformed or damaged shell, protruding mantle). The recorded endpoint was the percentage of normal D-larvae in each well respect to the total, including malformed larvae and pre-D stages. The acceptability of test results was based on controls fora percentage of normal D-shell stage larvae >75% (ASTM, 2004). Three experiments were made using 6 wells replicates per conditions. All larvae in each well were examined by optical microscopy using an inverted

Olympus IX53 microscope (Olympus, Milano, Italy) at 400x, equipped with a CCD UC30 camera and a digital image acquisition software (cellSens Entry).

*2.7. Statistics*

Data, representing the mean ± SD of 4 experiments, were analysed by ANOVA followed by Tukey's post-test ($p \leq 0.05$). For embryotoxicity test, data, representing the mean ± SD of 3 independent experiments, carried out in 6 replicates in 96-microwell plates. The $EC_{50}$ was defined as the concentration causing 50% reduction in the number of D-veligers at a 95% confidence interval (CI). All statistic calculations were performed by the PRISM 7 GraphPad software.

## 3. Results

*3.1 AgNP characterization*

In Fig.1 are reported the data on physico-chemical characterization of AgNP. Primary particle characterization showed that AgNPs are formed by irregular elongated polyhedrons and spherical particles with rounded and smooth edges (Fig. 1A, TEM images). The Z-average particle size obtained was 61 nm, with value ranging between 41 and 81 nm (64% of particles comprised between 35 and 65 nm) (Fig.1A distribution graph by frequency), very similar as the declared value (i.e. 40-90 nm). The sample presented little inorganic element impurities of Fe (24 ± 2 µg/g) and Ca (0.5 ± 0.1 µg/g) and a specific surface area obtained by BET method of 3.8 ± 0.1 $m^2$/ g. Characterization of particle suspensions in two exposure media (Fig.1B), ASW (10, 50, 100 mg/ L) and hemolymph serum (HS) (10 mg/L) was performed. DLS analysis of AgNPs in ASW showed the formation of two populations of agglomerates whose size increased with concentration (10, 50, 100 mg/L). Smaller agglomerates (138 ± 20; 130 ± 22; 340 ± 55 nm for each concentration respectively), represented less than a third of the whole population, whereas the majority was

represented by larger agglomerates (671 ± 122; 590 ± 99; 1600 ± 340 nm). A similar behaviour was observed for AgNP suspensions in HS (10 mg/L), with two populations of AgNPs, 89 ± 18 nm and 473 ± 57 nm, that were slightly smaller than those observed in ASW at the same concentration. Values of ζ-potential were similar at different concentrations in ASW (between -1.1 mv and -1.8 mV) and the same in both media at the same concentration (10 mg/L) (-1.5 ± 3.7 mV).

*3.2. Hemocyte functional responses*

The short term *in vitro* effects of different concentrations of AgNPs on *M. galloprovincialis* hemocytes were compared in ASW and HS, since different exposure media have been shown to influence the toxicity of certain types of NPs (Canesi et al., 2015, 2016, 2017). Hemocytes were exposed for 30 min to different concentrations (up to 1000 μg/mL) of AgNPs in ASW or HS and Lysosomal membrane stability (LMS) was first evaluated as a marker of cellular stress; the results are reported in Fig. 2. As shown in Fig. 2A, exposure of hemocytes to AgNPs in ASW induced a significant and concentration dependent decrease in LMS from 5 to 100 μg/mL (-17% to -38%, respectively; $P \leq 0.05$). A further decrease in LMS was observed at higher concentrations, together with cell detachment and death due to the presence of large agglomerates (not shown). A similar trend was observed for AgNP suspensions in HS. However, a slightly higher effect was observed with HS with respect to ASW only at 100 μg/mL (-50% in HS vs -38% in ASW; $P \leq 0.05$).

Exposure to $AgNO_3$ induced a sharp concentration-dependent decrease in LMS, that was significant from 0.5 μg/mL (-18% with respect to control; $P \leq 0.05$). A complete destabilization was observed at 2 μg/mL (Fig. 2B).

The distinct effects between AgNPs in ASW and $AgNO_3$were compared by evaluating their $EC_{50}$ values. For AgNP suspensions in ASW the $EC_{50}$ was 273.1 μg/mL (95% CI: 184.9-442.5 μg/mL). For $AgNO_3$ an $EC_{50}$ of 1.23 μg/mL (95% CI: 0.83-1.84 μg/mL) was obtained.

Due to the small difference in LMS observed in different exposure media, other parameters related to the immune function were measured using AgNP suspensions in ASW. AgNPs did not affect the phagocytic ability at any concentration tested from 5 to 100 µg/mL (Fig.3A). In contrast, $AgNO_3$ caused a concentration dependent decrease in phagocytic ability from 0.2 µg/mL ($P \leq 0.05$) (Fig. 3B). Neither AgNPs or $AgNO_3$, induced extracellular ROS release (data not shown).

*3.3 Effect on mitochondrial parameters and cytoskeleton*

The effects of hemocyte incubation with AgNPs (30 min) on mitochondria were evaluated by cell staining with TMRE (Tetramethylrhodamine, ethyl ester perchlorate) an indicator of mitochondrial membrane potential $\Delta\psi m$, and representative CLSM images are reported in Fig. 4. At lower concentrations (5 µg/mL) AgNPs did not affect TMRE fluorescence (not shown), whereas at 50 µg/mL a clear decrease was observed with respect to controls (Fig. 4A and B). AgNP agglomerates of different sizes (µm) were observed in the extracellular medium, with smaller agglomerates apparently taken up by the cells (Fig. 4B, right panel). Lower concentrations of $AgNO_3$ (0.2 µg/mL) were ineffective (not shown). However, at higher concentrations (1 µg/mL) $AgNO_3$ decreased TMRE fluorescence and induced cell rounding (Fig. 4C).

The effects of AgNPs on cytoskeletal structures of mussel hemocytes were evaluated by ActinGreen™488 staining, that reveals the architecture of cytosolic microfilaments, and representative CLSM images are shown in Fig. 5. Control hemocytes showed extended lamellipodia and cytoplasmic prolongations with the presence of thin microspikes, indicating strong adhesion to the substrate (Fig.5A). In hemocytes exposed to lower concentrations of AgNPs (5 and 10 µg/mL), a general decrease in the cytoplasmic signal was observed; however, cells retained their adherent shape, with evident microspikes (Fig.5B and 5C). In contrast, after exposure to higher concentrations (50 µg/mL), cells adopted a round shape with smaller cell extensions, and the actin

signal was often concentrated at the edge of the cells, close to the plasma membrane (Fig. 5D-F). In

hemocytes exposed to $AgNO_3$, a decrease in the cytoplasmic actin signal with respect to controls was observed at concentrations as low as 0.2 μg/mL, although cell morphology was unaffected (Fig.5G). At higher concentrations (1 μg/mL), $AgNO_3$ induced cell rounding and blebbing, indicating extensive cell damage and loss of adhesion (Fig. 5H).

*3.4 Embryotoxicity test*

Fertilized eggs were exposed to different concentrations (from 0.001 to 1000 μg/L) of AgNPs in 96-microwell plates, and the percentage of normal D-larvae was evaluated after 48 h as previously described (Fabbri et al., 2014; Balbi et al., 2017c). In controls, the percentage of normal D-larvae at 48 h was 82 ± 5%. The results, reported in Fig. 6, show that AgNPs induced a concentration-dependent decrease in normal larval development, with an $EC_{50}$= 23.7 μg/L (20.8 – 26.9 μg/L). The effect was significant from 10 μg/L (-30%; $P \leq 0.01$) and was dramatic (-75%) from concentrations ≥ 60 μg/L (Fig. 6A). As shown in Fig. 6B, at concentrations below $EC_{50}$, a concentration-dependent increase in malformed D-veligers was observed. A rise in the percentage of immature D-larvae and trocophorae was detected at higher concentrations. From concentrations of 80-100 μg/L, AgNPs completely inhibited the formation of the D-shaped veliger, with about 75% of the larvae withheld at the trocophora stage. Representative images of control and AgNPs-exposed larvae are reported in Fig. 6(C1-C3). Fig.6 C1 shows a normal D-veliger after 48h post fertilization with a characteristic D-shape. At 20 μg/L malformed larvae were observed (42% of total embryos); the characteristic D-shape was altered showing shell indentations and protruding mantle (Fig.6 C2). At higher concentrations (100 μg/L), larval development was delayed, with a majority of embryos at the trocophorae stage (C3).

The effects of $AgNO_3$ on embryo development were also evaluated, and the results are reported in Fig. 7. $AgNO_3$ induced a sharp concentration-dependent decrease in normal embryo development, with an $EC_{50}$ value of 1 μg/L (0.5 – 1.9 μg/L) (Fig. 7A), with most embryos showing

strong shell malformations (Fig. 7B). From 5 µg/L, no normal D-veligers were observed; $AgNO_3$ prevented development of fertilized eggs or resulted in dead trocophorae (not shown).

## 4. Discussion

Marine invertebrates can represent a significant target for the impact of nanosilver (Magesky and Pelletier, 2018), one of the most widespread NP type (Pulit-Prociak and Banach, 2016). In this work, data are presented on the effects of bare AgNPs (47 nm) in the marine bivalve *M. galloprovincialis* evaluated at the cellular and whole organism level using two model systems i.e. short term *in vitro* exposure of hemocytes and the 48 h embryotoxicity assay. The effects were compared with those of $AgNO_3$.

### *4.1 Effects on hemocytes*

High ionic strength media promote the formation of large AgNP agglomerates of several hundreds of nm, often represented by two main populations (Li et al., 2012; Yin et al., 2015). Accordingly, the results here presented show that in ASW AgNPs form large agglomerates of increasing size at increasing concentrations, with constant formation of two populations, the majority represented by larger agglomerates of hundred nms (Fig. 1). The results are comparable with other data on behaviour of different types of AgNPs in ASW (Sendra et al., 2017, Schiavo et al., 2017). No differences in ζ-potential were observed in ASW and HS, with values close to the point of zero charge (-1.5 ± 3.7 mV). Moreover, at 10 mg/L, agglomeration was lower in HS than in ASW: such an effect was previously observed with amino modified nanopolystyrene PS-$NH_2$ and $nCeO_2$ (Canesi et al., 2016; Canesi et al., 2017). These data indicate that in the experimental conditions utilized for most *in vitro* tests (≤ 100 µg/mL) the major part of AgNPs will be present in the form of agglomerates. Indeed, larger AgNP agglomerates of micrometric size were observed in the extracellular medium and smaller agglomerates were apparently internalized by hemocytes. These

observations are important for considering and understanding the response of hemocytes towards AgNPs. The results of functional parameters indicate little toxicity of AgNPs in mussel hemocytes. Although a concentration-dependent decrease in LMS was observed, from 5 μg/mL, $EC_{50}$ values were extremely high (273.1 μg/mL). Accordingly, no changes were observed in phagocytosis and extracellular ROS production at concentrations up to 100 μg/mL in both ASW and HS. The lack of disturbance of immune-related parameters suggests that in our experimental conditions AgNP agglomerates have little interactions at the level of the cell membrane. The results are in line with those previously obtained in cells from *M. galloprovincialis* exposed to maltose-coated AgNPs for longer periods of time (Katsumiti et al., 2015). As to the possible uptake of AgNPs or AgNP agglomerates, this could fairly occur during the 30 min incubation by phagocytosis. However, preliminary TEM observations indicate little intracellular uptake of AgNPs.

In this work, the effects of AgNPs were also investigated in the presence of different exposure media (in ASW and HS). The importance of the exposure media has been emphasized when testing NPs in different cell models, including mussel hemocytes (Ren et al., 2016; Canesi et al., 2017). Data on identification of NP protein coronas for PS-$NH_2$ and $nCeO_2$ suggested that the net surface charge retained by the particles in high ionic strength media, such as mussel hemolymph, might be an important factor in the formation of a stable protein corona, that can increase or decrease particle interactions with hemocytes (Canesi et al. 2017). The results here obtained seem to reinforce this hypothesis: AgNPs displayed a quasi-neutral surface charge in both ASW and HS, and the presence of HS had little effect on lysosomal membrane stability, indicating that interactions with protein serum components seem to little affect the response of hemocyte to AgNPs.

AgNPs are known to be highly corroded in presence of salts and oxygen and can release silver ions ($Ag^+$) in high ionic strength media like ASW (Liu and Hurt, 2010; Levard et al., 2012). Although Ag solubility may be different in ASW and HS, the similar hemocyte responses observed in the two media suggest that differences in Ag dissolution in relation to toxicity may be negligible.

On the other hand, available data from exposure experiments of cells from marine organisms are on Ag dissolution in standard AgNP suspensions in SW, and not in the actual exposure media specific for each cell type (mussel cells or unicellular algae) (Katsumiti et al., 2015; Schiavo et al., 2017). In this light, determination of dissolution of meal based NPs in actual exposure media for *in vitro* experiments using different models of cells from marine organisms represents a general problem that has not been addressed so far, and that would require a detailed analytical investigation.

In order to investigate the complementary role of ions released from NPs, parallel experiments were performed using silver nitrate ($AgNO_3$) to evaluate the effects of $Ag^+$ in its soluble form. $AgNO_3$ induced a dramatic decrease in LMS, with an $EC_{50}$as low as 1 µg/mL. Moreover, in the same concentration range, $AgNO_3$ induced a concentration-dependent inhibition of the phagocytic activity. These data indicate a much stronger and distinct effect of $Ag^+$ in comparison with AgNPs in mussel hemocytes.

In mussels, *in vitro* and *in vivo* studies have shown that the immune system represents a sensitive target for different types of NPs. In particular, the application of a battery of functional tests on *Mytilus* hemocytes, as a cell model of marine organisms, has proven as a powerful tool for the rapid *in vitro* screening of the immunomodulatory effects of different types of NPs (Canesi et al., 2012; Canesi and Procházková, 2013, Canesi and Corsi et al., 2016). Induction of functional responses, as well as of cellular damage and apoptotic processes, were particularly rapid, occurring within 1 h of exposure, in line with the physiological role of bivalve hemocytes as the first line of defence against non-self material (Canesi et al., 2017 and refs. quoted therein). In short term exposure experiments NPs rapidly affected different parameters related to lysosomal function, phagocytosis, oxyradical production, apoptosis, with LMS being considered the most sensitive endpoint (Canesi et al., 2012; Canesi and Procházková, 2013, Canesi and Corsi et al., 2016). However, certain NP types (nanosized carbon black-NCB, PS-$NH_2$ and n-ZnO) have been shown to affect also mitochondrial parameters and pre-apoptotic processes (Canesi et al., 2008, 2015; Ciacci et al., 2012).

The results here presented show that AgNPs induced a rapid decrease in mitochondrial membrane potential at 50 µg/mL, a concentration much lower than the $EC_{50}$ for LMS. Alteration of $_{\Psi}\Delta m$ by AgNPs was recorded for several mammalian and human cells (Asharani et al., 2009; Singh and Romarao 2012; Yang et al., 2012). AgNPs can strongly interact with membrane thiol groups (-SH) and stay immobilized near the membrane, including the mitochondrial membrane, where they can interfere with protons present in the intermembrane space thus affecting the electron flow and possibly enhancing the formation of ROS (Lapestra-Fernandez et al., 2012; Yang et al., 2012; Zhang et al., 2014). Also exposure to $AgNO_3$ reduced mitochondrial membrane potential, although at much lower concentrations; a clear decrease in TMRE fluorescence accompanied by cell rounding was observed at 1 µg/mL, thus paralleling the effects on lysosomal membranes.

AgNPs also affected hemocyte cytoskeletal structures, with a decrease in immunofluorescence of filamentous actin from 5 µg/mL; at higher concentrations (50 µg/mL), morphological changes were also observed, with cells adopting a round shape with smaller extensions; moreover, a concentration of the actin signal in the peripheral part of the cells was observed. The effects of AgNPs on cytoskeletal structures are in line with previous data obtained both in mussel hemocytes (Katsumiti et al., 2015) and in human cells (Zhao et al., 2017), although at longer exposure time (hours). Cytoskeletal alterations induced by AgNPs may be ascribed to AgNP dissolution; $Ag^+$ ions may act directly, by binding to actin filaments causing depolymerisation, or indirectly, through alterations of $Ca^{2+}$ homeostasis, mitochondrial damage and ROS production (Asharani et al., 2009; Singh and Romarao 2012; Gomes et al., 2013; Zhao et al., 2017). However, AgNPs show a strong binding capacity for both actin and tubulin *in vitro*, altering secondary structures of the proteins and in particular perturbing the structural integrity of the alpha helices of actin (Wen et al., 2013). The results here obtained indicate that the effects of AgNPs on actin cytoskeleton in mussel hemocytes are extremely rapid, occurring at 30 min of exposure and at concentrations that did not cause strong lysosomal damage or impairment of immune parameters. In

contrast, $AgNO_3$ severely affected actin cytoskeleton, and induced cell rounding at much lower

concentrations (0.2-1 μg/mL), in parallel with decreased in LMS and phagocytic activity, indicating extensive cellular damage.

*4.2. Effects on embryo development*

For environmental regulatory purposes, data on early life stages of aquatic species are important to establish the sensitivity of a species to different contaminants. The 48 h bivalve embryotoxicity test represents a standardized and reproducible protocol that allows the sensitive evaluation of the early developmental effects of a number of both legacy and emerging pollutants (ASTM, 2004, ASTM, 2012; Fabbri et al., 2014).

The present results demonstrate that AgNPs significantly affect *M. galloprovincialis* early development. A sharp concentration-dependent decrease in the percentage of normal embryos was recorded in a narrow concentration range (10-100 μg/L), with an $EC_{50}$ of 23.7 μg/L. At lower concentrations, the characteristic D-shape of embryos was altered, showing shell indentations and protruding mantle. Moreover, from 40 μg/L, an increase in immature embryos was observed, indicating progressive developmental arrest. Similarly, embryos of the oyster *Crassostrea virginica* exposed to AgNPs of smaller size (15 nm) showed a decrease in normal development; the effects were observed at low μg/L concentrations, although particle behaviour and type of developmental effect were not evaluated (Ringwood et al., 2010). Higher concentrations (300 μg/L) of citrate stabilized AgNPs (5-35 nm) have been shown to induce developmental toxicity in the sea urchin *Paracentrotus lividus* at 48 hpf. (Šiller et al., 2013). All together, these data suggest that different types of AgNPs may have a significant impact on embryo development in marine invertebrates.

Moreover, our data show that in *M. galloprovincialis* embryos AgNPs had stronger detrimental effects compared to other types of NPs. Exposure to stabilized zero-valent nanoiron (nZVI) resulted in a decrease in normal D-shaped mussel embryos, with significant effects from concentrations ≤ 100 μg/L (Kadar et al., 2011). In contrast, n-$TiO_2$ did not affect embryo

development at concentrations lower than 4 mg/L (Libralato et al., 2012; Balbi et al., 2014). Similarly, $nCeO_2$ was ineffective up to 1 mg/L (Canesi, unpublished results).

When the embryotoxicity of ionic $Ag^+$ was evaluated using $AgNO_3$, obtained $EC_{50}$ values (1 µg/L) were more than twenty times lower than that of AgNPs and similar to that induced by $Cu^{2+}$, the reference metal used as positive control in the embryotoxicity assay (Fabbri et al., 2014). In comparison with short term *in vitro* tests with hemocytes, the effects of AgNPs over the time course of the embryotoxicity assay (48 h) may be the result of metal dissolution in ASW, as shown for different types of AgNPs, depending on particle size, agglomeration, pH and coating, with smaller and coated AgNPs releasing more $Ag^+$ (Katsumiti et al., 2015; Schiavo et al., 2017; Sendra et al., 2017). Although in the present study the release of $Ag^+$ was not evaluated, Schiavo et al. (2017) showed that for the same AgNP type (uncoated 47nm AgNPs) released $Ag^+$ in ASW was about 0.6-1.5- 3% at 0, 24 and 48 h, respectively. If this were the case, at the $EC_{50}$ for AgNPs of 23.7 µg/L embryos would be exposed to a maximum of 0.7 µg/L $Ag^+$ at the end of the assay (48 h) and to much lower concentrations at shorter times of exposure (0.14, 0.35 µg/L, respectively, for fertilized eggs and trocophorae at 0 and 24 h pf). The lower impact of AgNP on embryos compared to $AgNO_3$ could be related to the limited amount of bioavailable nanomaterial due to high agglomeration state of AgNPs in ASW. Moreover, the type of effects of AgNPs on embryo development were distinct from those of ionic $Ag^+$. AgNPs caused malformations and developmental delay, but no mortality, in a wide concentration range, whereas $AgNO_3$ mainly induced shell malformations followed by developmental arrest or death.

## 5. Conclusions

The data reported in the present study represent a first attempt to compare the possible effects and mechanism of action of AgNPs and soluble $Ag^+$ in mussels at the cellular and organism level. In both experimental settings, AgNPs was effective at much higher concentrations that those

of $AgNO_3$, indicating little toxicity; moreover, the mechanisms of action of AgNPs appeared to be distinct from those of $Ag^+$ in both hemocytes and embryos. The lower toxicity of AgNPs may be partly due to agglomeration. In addition, characterisation of Ag speciation in experimental media is critical for mechanistically linking AgNP dissolution to toxicity (Lodeiro et al., 2017). Alongside physicochemical processes, investigation of the speciation and biotransformation is also important for understanding physiological, biochemical, and molecular modifications induced by exposure by AgNPs in marine organisms (Wang et al., 2015; Magesky and Pelletier 2018). In polychaetes, chronic exposure to different types of AgNPs results in the formation of different amounts Ag metal and AgCl, apparently depending on the original form of silver to which the worms were exposed, in particular to the type of coating, with citrate-AgNPs also resulting in the formation of $Ag_2S$ (Wang et al., 2015). Moreover, Ag sulfidation in exposure media has been shown to decrease the toxicity of AgNPs in aquatic and terrestrial organisms (Levard et al., 2013). However, no information is available on the protective effects of $Ag_2S$ in marine organisms. Although determination of Ag speciation in either exposure media and within cells/embryos was outside of the scope of the present work, it may contribute to explain the effects of AgNPs.

Overall, the results provide a further insight into the effects and mechanisms of action of AgNPs in marine invertebrates. According to the results of a recent study, engineered nanomaterials pose relatively low risk for most environmental compartments (Giese et al., 2018); in particular, for AgNPs, the PECs for marine waters reveal present values below pg/l levels and, in 2050, up to 1 pg/l, much lower than those utilized in the present work and in available literature on the effects of AgNPs in marine organisms. However, as underlined by Giese et al. (2018), organisms residing near 'point sources' (e.g., production plant outfalls and waste treatment plants), may be at increased risk; this may apply to marine mussels living in such coastal and estuarine environments.



**Funding**

This project has received funding from the European Union's Horizon 2020 research and innovation programme under the Marie Skłodowska-Curie grant agreement PANDORA N° 671881.

## References

Asharani, P.V., Low KahMun, G., Hande, M.P., Valiyaveettil, S., 2009. Cytotoxicity and Genotoxicity of Silver Nanoparticles in Human Cells. ACS Nano 3, 279–290. https://doi.org/10.1021/nn800596w

ASTM, 2004. Standard Guide for Conducting Static Acute Toxicity Tests Starting with Embryos of Four Species of Saltwater Bivalve Molluscs. http://dx.doi.org/10.1520/E0724-98.

ASTM, 2012. Standard Guide for Conducting Static Acute Toxicity Tests Starting with Embryos of Four Species of Saltwater Bivalve Molluscs.http://dx.doi.org/10.1520/E0724-98R12

ASTM D1141-98, 2013. Standard Practice for the Preparation of Substitute Ocean Water, https://doi.org/10.1520/D1141-98R13

Balbi, T., Caratto, V., Fabbri, R., Camisassi, G., Villa, S., Ferretti, M., Canesi, L., 2017a. Photocatalytic Fe-doped n-$TiO_2$: From synthesis to utilization of *in vitro* cell models for screening human and environmental nanosafety. Resource-Efficient Technologies 3, 158–165. https://doi.org/10.1016/j.reffit.2017.03.009

Balbi, T., Fabbri, R., Montagna, M., Camisassi, G., Canesi, L., 2017b. Seasonal variability of different biomarkers in mussels (*Mytilus galloprovincialis*) farmed at different sites of the Gulf of La Spezia, Ligurian sea, Italy. Mar Pollut Bull 116, 348–356. https://doi.org/10.1016/j.marpolbul.2017.01.035

Balbi, T., Camisassi, G., Montagna, M., Fabbri, R., Franzellitti, S., Carbone, C., Dawson, K., Canesi, L., 2017c. Impact of cationic polystyrene nanoparticles (PS-$NH_2$) on early embryo development of *Mytilus galloprovincialis*: Effects on shell formation. Chemosphere 186, 1–9. https://doi.org/10.1016/j.chemosphere.2017.07.120

Balbi, T., Smerilli, A., Fabbri, R., Ciacci, C., Montagna, M., Grasselli, E., Brunelli, A., Pojana, G., Marcomini, A., Gallo, G., Canesi, L., 2014. Co-exposure to n-$TiO_2$ and $Cd^{2+}$ results in interactive effects on biomarker responses but not in increased toxicity in the marine bivalve *M. galloprovincialis*. Sci Total Environ 493, 355–364. https://doi.org/10.1016/j.scitotenv.2014.05.146

Beyer, J., Green, N.W., Brooks, S., Allan, I.J., Ruus, A., Gomes, T., Bråte, I.L.N., Schøyen, M., 2017. Blue mussels (*Mytilus edulis* spp.) as sentinel organisms in coastal pollution monitoring: A review. Mar Environ Res 130, 338–365. https://doi.org/10.1016/j.marenvres.2017.07.024

Brunelli, A., Pojana, G., Callegaro, S., Marcomini, A., 2013. Agglomeration and sedimentation of titanium dioxide nanoparticles (n-$TiO_2$) in synthetic and real waters. J Nanopart Res 15. https://doi.org/10.1007/s11051-013-1684-4

Brunelli Andrea, 2013 «Advanced physico-chemical characterization of engineered nanomaterials in nanotoxicology», PhD Thesis, University Ca' Foscari Venice, Italy; 172 p.

Canesi, L., Ciacci, C., Betti, M., Fabbri, R., Canonico, B., Fantinati, A., Marcomini, A., Pojana, G., 2008. Immunotoxicity of carbon black nanoparticles to blue mussel hemocytes. Environ Int 34, 1114–1119. https://doi.org/10.1016/j.envint.2008.04.002

Canesi, L., Ciacci, C., Vallotto, D., Gallo, G., Marcomini, A., Pojana, G., 2010. *In vitro* effects of suspensions of selected nanoparticles (C60 fullerene, $TiO_2$, $SiO_2$) on *Mytilus* hemocytes. Aquat Toxicol 96, 151–158. https://doi.org/10.1016/j.aquatox.2009.10.017

Canesi, L., Ciacci, C., Fabbri, R., Marcomini, A., Pojana, G., Gallo, G., 2012. Bivalve molluscs as a unique target group for nanoparticle toxicity. Mar Environ Res 76, 16–21. https://doi.org/10.1016/j.marenvres.2011.06.005

Canesi L. and Procházová P., 2013. The invertebrate immune system as a model for investigating the environmental impact of nanoparticles, in: Boraschi D, Duschl A, (Eds.), Nanoparticles and the immune system. Oxford Academic Press, pp. 91-112.

Canesi, L., Ciacci, C., Bergami, E., Monopoli, M.P., Dawson, K.A., Papa, S., Canonico, B., Corsi, I., 2015. Evidence for immunomodulation and apoptotic processes induced by cationic polystyrene nanoparticles in the hemocytes of the marine bivalve *Mytilus*. Mar Environ Res 111, 34–40. https://doi.org/10.1016/j.marenvres.2015.06.008

Canesi, L., Ciacci, C., Balbi, T., 2016. Invertebrate Models for Investigating the Impact of Nanomaterials on Innate Immunity: The Example of the Marine Mussel *Mytilus spp*. Current Bionanotechnol 2, 77–83. https://doi.org/10.2174/2213529402666160601102529

Canesi, L. andCorsi, I., 2016. Effects of nanomaterials on marine invertebrates. Sci Total Environ 565, 933–940. https://doi.org/10.1016/j.scitotenv.2016.01.085

Canesi, L., Balbi, T., Fabbri, R., Salis, A., Damonte, G., Volland, M., Blasco, J., 2017. Biomolecular coronas in invertebrate species: Implications in the environmental impact of nanoparticles. NanoImpact 8, 89–98. https://doi.org/10.1016/j.impact.2017.08.001

Ciacci, C., Canonico, B., Bilaniĉovă, D., Fabbri, R., Cortese, K., Gallo, G., Marcomini, A., Pojana, G., Canesi, L., 2012. Immunomodulation by Different Types of N-Oxides in the Hemocytes of the Marine Bivalve *Mytilus galloprovincialis*. PLoS ONE 7, e36937. https://doi.org/10.1371/journal.pone.0036937

Fabbri, R., Montagna, M., Balbi, T., Raffo, E., Palumbo, F., Canesi, L., 2014. Adaptation of the bivalve embryotoxicity assay for the high throughput screening of emerging contaminants in *Mytilus galloprovincialis*. Marine Environmental Research 99, 1–8. https://doi.org/10.1016/j.marenvres.2014.05.007

Fabrega, J., Luoma, S.N., Tyler, C.R., Galloway, T.S., Lead, J.R., 2011. Silver nanoparticles: Behaviour and effects in the aquatic environment. Environ Int 37, 517–531. https://doi.org/10.1016/j.envint.2010.10.012

Faggio, C., Tsarpali, V., Dailianis, S., 2018. Mussel digestive gland as a model tissue for assessing xenobiotics: An overview. Sci Total Environ 636, 220–229. https://doi.org/10.1016/j.scitotenv.2018.04.264

Giese, B., Klaessig, F., Park, B., Kaegi, R., Steinfeldt, M., Wigger, H., von Gleich, A., Gottschalk, F., 2018. Risks, Release and Concentrations of Engineered Nanomaterial in the Environment. Sci Rep 8. https://doi.org/10.1038/s41598-018-19275-4

Gomes, T., Pereira, C.G., Cardoso, C., Bebianno, M.J., 2013. Differential protein expression in mussels *Mytilus galloprovincialis* exposed to nano and ionic Ag. Aquat Toxicol 136–137, 79–90. https://doi.org/10.1016/j.aquatox.2013.03.021

Gottschalk, F., Sonderer, T., Scholz, R.W., Nowack, B., 2009. Modeled environmental concentrations of engineered nanomaterials ($TiO_2$, ZnO, Ag, CNT, fullerenes) for different regions. Environ Sci Technol 43, 9216–9222.

Jemec, A., Kahru, A., Potthoff, A., Drobne, D., Heinlaan, M., Böhme, S., Geppert, M., Novak, S., Schirmer, K., Rekulapally, R., Singh, S., Aruoja, V., Sihtmäe, M., Juganson, K., Käkinen, A., Kühnel, D., 2016. An interlaboratory comparison of nanosilver characterisation and hazard identification: Harmonising techniques for high quality data. Environ Int 87, 20–32. https://doi.org/10.1016/j.envint.2015.10.014

Jimeno-Romero, A., Bilbao, E., Izagirre, U., Cajaraville, M.P., Marigómez, I., Soto, M., 2017. Digestive cell lysosomes as main targets for Ag accumulation and toxicity in marine mussels, *Mytilus galloprovincialis*, exposed to maltose-stabilised Ag nanoparticles of different sizes. Nanotoxicology 11, 168–183. https://doi.org/10.1080/17435390.2017.1279358

Kadar, E., Tarran, G.A., Jha, A.N., Al-Subiai, S.N., 2011. Stabilization of Engineered Zero-Valent Nanoiron with Na-Acrylic Copolymer Enhances Spermiotoxicity. Environ Sci Technol 45, 3245–3251. https://doi.org/10.1021/es1029848

Katsumiti, A., Gilliland, D., Arostegui, I., Cajaraville, M.P., 2015. Mechanisms of Toxicity of Ag Nanoparticles in Comparison to Bulk and Ionic Ag on Mussel Hemocytes and Gill Cells. PLOS ONE 10, e0129039. https://doi.org/10.1371/journal.pone.0129039

Lapresta-Fernández, A., Fernández, A., Blasco, J., 2012. Nanoecotoxicity effects of engineered silver and gold nanoparticles in aquatic organisms. TrAC 32, 40–59. https://doi.org/10.1016/j.trac.2011.09.007

Levard, C., Hotze, E.M., Lowry, G.V., Brown, G.E., 2012. Environmental Transformations of Silver Nanoparticles: Impact on Stability and Toxicity. Environ Sci Technol 46, 6900–6914. https://doi.org/10.1021/es2037405

Levard, C., Hotze, E.M., Colman, B.P., Dale, A.L., Truong, L., Yang, X.Y., Bone, A.J., Brown, G.E., Tanguay, R.L., Di Giulio, R.T., Bernhardt, E.S., Meyer, J.N., Wiesner, M.R., Lowry, G.V., 2013. Sulfidation of Silver Nanoparticles: Natural Antidote to Their Toxicity. Env Sci Technol 47, 13440–13448. https://doi.org/10.1021/es403527n

Li, X., Lenhart, J.J., Walker, H.W., 2012. Aggregation Kinetics and Dissolution of Coated Silver Nanoparticles. Langmuir 28, 1095–1104. https://doi.org/10.1021/la202328n

Li, L., Wu, H., Peijnenburg, W.J., van Gestel, C.A., 2014. Both released silver ions and particulate Ag contribute to the toxicity of AgNPs to earthworm *Eisenia fetida*, Nanotoxicology, 9:6, 792-801, https://doi.org/10.3109/17435390.2014.976851

Libralato, G., Minetto, D., Totaro, S., Mičetić, I., Pigozzo, A., Sabbioni, E., Marcomini, A., Volpi Ghirardini, A., 2013. Embryotoxicity of $TiO_2$ nanoparticles to *Mytilus galloprovincialis* (Lmk). Mar Environ Res 92, 71–78. https://doi.org/10.1016/j.marenvres.2013.08.015

Liu, J. and Hurt, R.H., 2010. Ion Release Kinetics and Particle Persistence in Aqueous Nano-Silver Colloids. Environ SciTechnol 44, 2169–2175. https://doi.org/10.1021/es9035557

Lodeiro, P., Browning, T.J., Achterberg, E.P., Guillou, A., El-Shahawi, M.S., 2017. Mechanisms of silver nanoparticle toxicity to the coastal marine diatom *Chaetoceros curvisetus*. Sci Rep 7. https://doi.org/10.1038/s41598-017-11402-x

McCarthy, M.P., Carroll, D.L., Ringwood, A.H., 2013. Tissue specific responses of oysters, *Crassostreavirginica*, to silver nanoparticles. AquatToxicol 138–139, 123–128. https://doi.org/10.1016/j.aquatox.2013.04.015

McGillicuddy, E., Murray, I., Kavanagh, S., Morrison, L., Fogarty, A., Cormican, M., Dockery, P., Prendergast, M., Rowan, N., Morris, D., 2017. Silver nanoparticles in the environment: Sources, detection and ecotoxicology. Sci Total Environ 575, 231–246. https://doi.org/10.1016/j.scitotenv.2016.10.041

Magesky, A., Pelletier, E., 2018. Cytotoxicity and Physiological Effects of Silver Nanoparticles on Marine Invertebrates, in: Saquib, Q., Faisal, M., Al-Khedhairy, A.A., Alatar, A.A., (Eds.), Cellular and Molecular Toxicology of Nanoparticles. Springer International Publishing, pp.285-309. https://doi.org/10.1007/978-3-319-72041-8

Pulit-Prociak, J., Banach, M., 2016. Silver nanoparticles – a material of the future…? Open Chem14. https://doi.org/10.1515/chem-2016-0005

Ren, C., Hu, X., Zhou, Q., 2016. Influence of environmental factors on nanotoxicity and knowledge gaps thereof. NanoImpact 2, 82–92. https://doi.org/10.1016/j.impact.2016.07.002

Ringwood, A.H., McCarthy, M., Bates, T.C., Carroll, D.L., 2010. The effects of silver nanoparticles on oyster embryos. Mar Environ Res 69, S49–S51. https://doi.org/10.1016/j.marenvres.2009.10.011 Rocha, T.L., Gomes, T., Sousa, V.S., Mestre, N.C., Bebianno, M.J., 2015. Ecotoxicological impact of engineered nanomaterials in bivalve molluscs: An overview. Mar Environ Res 111, 74–88. https://doi.org/10.1016/j.marenvres.2015.06.013

Schiavo, S., Duroudier, N., Bilbao, E., Mikolaczyk, M., Schäfer, J., Cajaraville, M.P., Manzo, S., 2017. Effects of PVP/PEI coated and uncoated silver NPs and PVP/PEI coating agent on three species of marine microalgae. Sci Total Environ 577, 45–53. https://doi.org/10.1016/j.scitotenv.2016.10.051

Sendra, M., Yeste, M.P., Gatica, J.M., Moreno-Garrido, I., Blasco, J., 2017. Direct and indirect effects of silver nanoparticles on freshwater and marine microalgae (*Chlamydomonas reinhardtii* and *Phaeodactylum tricornutum*). Chemosphere 179, 279–289. https://doi.org/10.1016/j.chemosphere.2017.03.123

Šiller, L., Lemloh, M.-L., Piticharoenphun, S., Mendis, B.G., Horrocks, B.R., Brümmer, F., Medaković, D., 2013. Silver nanoparticle toxicity in sea urchin*Paracentrotus lividus*. Environ Pollut 178, 498–502. https://doi.org/10.1016/j.envpol.2013.03.010

Singh, R.P., Ramarao, P., 2012. Cellular uptake, intracellular trafficking and cytotoxicity of silver nanoparticles. Toxicol Lett 213, 249–259. https://doi.org/10.1016/j.toxlet.2012.07.009

Wang, H., Ho, K.T., Scheckel, K.G., Wu, F., Cantwell, M.G., Katz, D.R., Horowitz, D.B., Boothman, W.S., Burgess, R.M., 2014. Toxicity, Bioaccumulation, and Biotransformation of Silver Nanoparticles in Marine Organisms. Environ Sci Technol 48, 13711–13717. https://doi.org/10.1021/es502976y

Wen, Y., Geitner, N.K., Chen, R., Ding, F., Chen, P., Andorfer, R.E., Govindan, P.N., Ke, P.C., 2013. Binding of cytoskeletal proteins with silver nanoparticles. RSC Advances 3, 22002. https://doi.org/10.1039/c3ra43281e

Yang, E.-J., Kim, S., Kim, J.S., Choi, I.-H., 2012. Inflammasome formation and IL-1β release by human blood monocytes in response to silver nanoparticles. Biomaterials 33, 6858–6867. https://doi.org/10.1016/j.biomaterials.2012.06.016

Yin, Y., Yang, X., Zhou, X., Wang, W., Yu, S., Liu, J., Jiang, G., 2015. Water chemistry controlled aggregation and photo-transformation of silver nanoparticles in environmental waters. J Environ Sci 34, 116–125. https://doi.org/10.1016/j.jes.2015.04.005

Zhang, T., Wang, L., Chen, Q., Chen, C., 2014. Cytotoxic Potential of Silver Nanoparticles. Yonsei Med J 55, 283. https://doi.org/10.3349/ymj.2014.55.2.283

Zhao, X., Toyooka, T., Ibuki, Y., 2017. Silver nanoparticle-induced phosphorylation of histone H3 at serine 10 is due to dynamic changes in actin filaments and the activation of Aurora kinases. Toxicol Lett 276, 39–47. https://doi.org/10.1016/j.toxlet.2017.05.009

Zuykov, M., Pelletier, E., Demers, S., 2011. Colloidal complexed silver and silver nanoparticles in extrapallial fluid of *Mytilus edulis*. Mar Environ Res 71, 17–21. https://doi.org/10.1016/j.marenvres.2010.09.004

**Figures captions**

**Figure 1** -Physico-chemical characterization of bare 47 nm AgNPs (Inframat® Advanced Materials).

A) Primary particle characterization. Top left: Z-average (nm), inorganic element impurities evaluated by ICP-OES and specific surface area by BET method. Bottom left: Particle size distribution graph by frequency. Right: TEM images.

B) Characterization of AgNP suspensions in artificial seawater (ASW) and *Mytilus* hemolymph serum (HS), using DLS analysis showing Z-average (nm) and ζ-potential (mV). Data are reported as mean ± SD.

**Figure 2-** Effects of AgNPs and $AgNO_3$ on Lysosomal membrane stability (LMS) of *Mytilus* hemocytes. Hemocytes were exposed for 30 min to different concentrations of AgNPs and LMS was evaluated by the NRR time assay (A). AgNP suspensions in either ASW or hemolymph serum (HS) were utilized. Parallel experiments were carried out using different concentrations of $AgNO_3$ diluted in ASW (B). Data, representing the mean ± SD of four experiments in triplicate, were analysed by ANOVA followed by Tukey's post hoc test ($p < 0.05$); * = all treatments vs controls; # = HS vs ASW.

**Figure 3-**Effects of AgNPs and $AgNO_3$in ASW on phagocytic activity of *Mytilus* hemocytes, A) AgNPs; B) $AgNO_3$. Data, representing the mean ± SD of three experiments in triplicate, were analysed by ANOVA followed by Tukey's post hoc test. Significant differences with respect to controls ($p < 0.05$) are reported (*).

**Figure 4 -** Confocal fluorescence microscopy: effects of exposure of *Mytilus* hemocytes to AgNPs and $AgNO_3$ (30 min)on mitochondrial membrane potential ($\Delta\Psi m$)evaluated by TMRE fluorescence. Control and treated hemocytes were loaded with TMRE (and representative images are reported (568 excitation/ 590-630 emission) (Left panels). A) Control hemocytes; B) hemocytes exposed to AgNPs (50 µg/mL); C) hemocytes exposed to $AgNO_3$: 0.2 µg/mL. In right panels, light microscopy images are also reported: B) shows the presence of large AgNP agglomerates in the extracellular medium (arrowheads) and of smaller agglomerates apparently taken up by the cells (arrows). In C), cell rounding induced by $AgNO_3$ can be observed. Scale bar: 25 µm.

**Figure 5 -**Confocal fluorescence microscopy: effects of exposure of *Mytilus* hemocytes to AgNPs and $AgNO_3$ (30 min)on actin cytoskeleton. Control and treated hemocytes were loaded with ActinGreen™488 and representative images are reported (495 excitation/518 emission): A) Control hemocytes; B-F) hemocytes exposed to AgNPs: B) 5 µg/mL, C) 10 µg/ml and D-F) 50 µg/mL; G-H)Hemocytes exposed to $AgNO_3$ : G) 0.2 µg/mL and H) 1 µg/mL. Scale bar: 25µm.

**Figure 6 -** Effects of AgNPs on *M. galloprovincialis* larval development evaluated in the 48 h embryotoxicity assay. Fertilized eggs were exposed to different concentrations of AgNPs in ASW (0.001-1000 µg/L).

A) Percentage of normal D-shaped larvae with respect to controls. The $EC_{50}$ reported for AgNP exposure was 23.7 µg/L. B) Percentage of normal D-veliger (white), malformed D-veliger (grey), pre-veligers (black) and trocophora (shaded) in each experimental condition. C1-C3: Representative light microscopy images of control and AgNP-exposed embryos: C1) a normal D-larva; C2) a malformed D-larva showing shell indentations (arrowheads) and protruding mantle (arrow) in samples exposed to 20 µg/L AgNPs; C3) an immature embryo withheld at the trocophora stage in samples exposed to 100 µg/L AgNPs. Scale bars: 20 µm. Data represent the mean ± SD of 3 experiments carried out in 96-multiwell plates (6 replicate wells for each sample).

**Figure 7 -** Effects of $AgNO_3$ on *M. galloprovincialis* larval development in the 48 h embryotoxicity assay. Fertilized eggs were exposed to different concentrations of $AgNO_3$ (0.1-25 µg/L). A) Percentage of normal D-shaped larvae with respect to controls. The $EC_{50}$ reported for $AgNO_3$ exposure was 1 µg/L. B) Representative light microscopy image of a malformed D-larva exposed to

5 µg/L $AgNO_3$. Scale bar: 20 µm. Data, representing the mean ± SD of 3 experiments carried out in 96-multiwell plates (6 replicate wells for each sample).

**A**

| Z-average (nm) | Inorganic impurities by ICP-OES (µg/g) | Surface area by BET ($m^2/g$) |
|---|---|---|
| 61 ± 20 | Fe: 24 ± 2 (LOD: 0.6)<br>Ca: 0.5 ± 0.1 (LOD: 0.03) | 3.8 ± 0.1 |

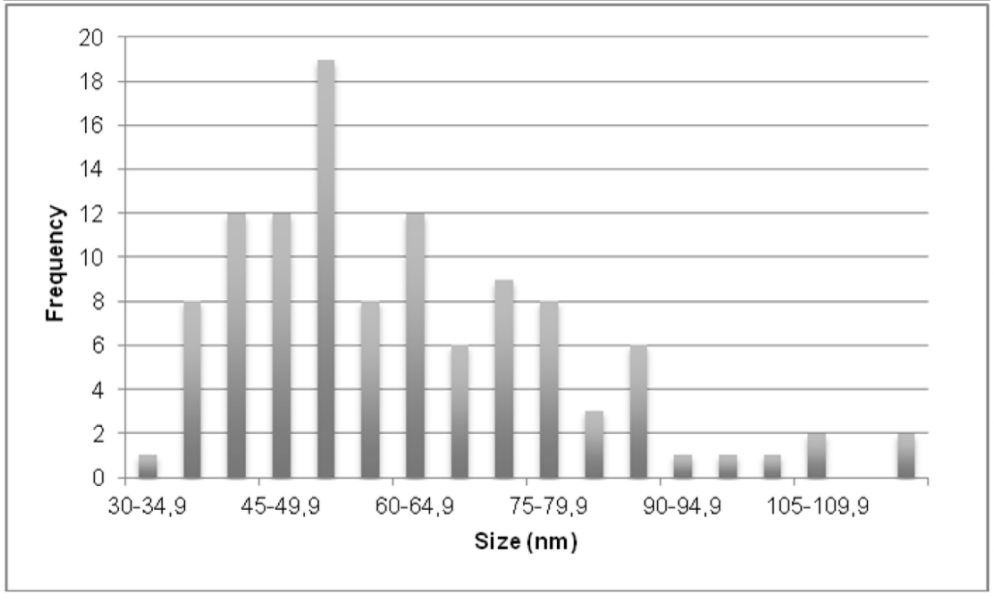


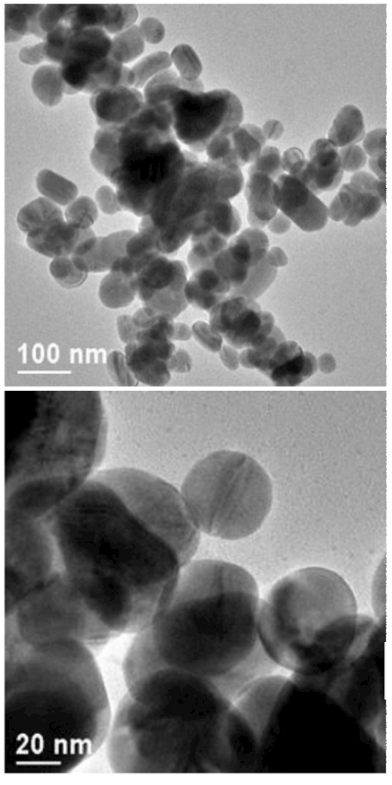


**B**

| **AgNPs** Particle suspension | | Z-average (nm) | ζ-potential (mV) |
|---|---|---|---|
| ASW | 10 mg/L | 138 ± 20 (25%)<br>671 ± 122 (75%) | -1.5 ± 3.7 |
| | 50 mg/L | 130 ± 22 (15%)<br>590 ± 99 (85%) | -1.1 ± 2.3 |
| | 100 mg/L | 340 ± 55 nm (28%)<br>1600 ± 340 nm (72%) | -1.8 ± 1.9 |
| HS | 10 mg/L | 89 ± 18 (20%)<br>473 ± 57 (80%) | -1.5 ± 3.7 |

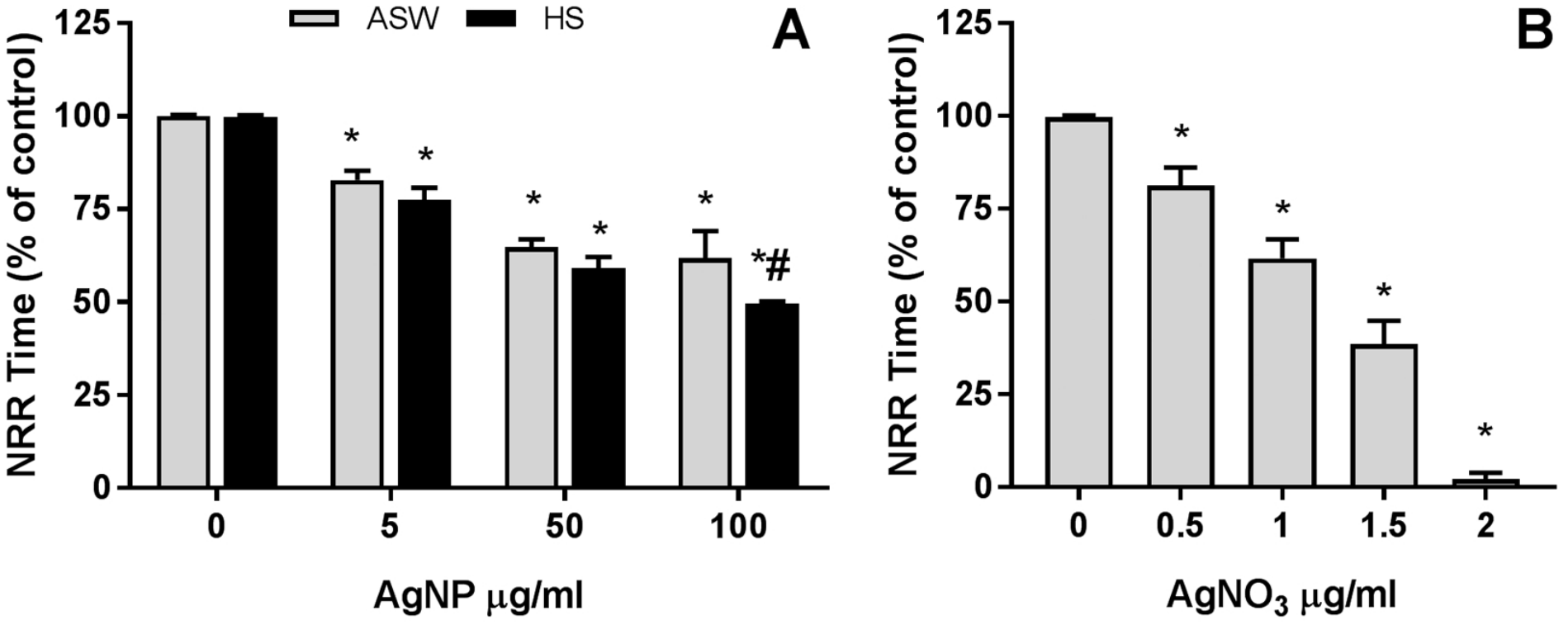
A
ASW
HS
NRR Time (% of control)
125
100
75
50
25
0
0
5
50
100
AgNP μg/ml
*
*
*
*
*
*#
B
NRR Time (% of control)
125
100
75
50
25
0
0
0.5
1
1.5
2
AgNO3 μg/ml
*
*
*
*

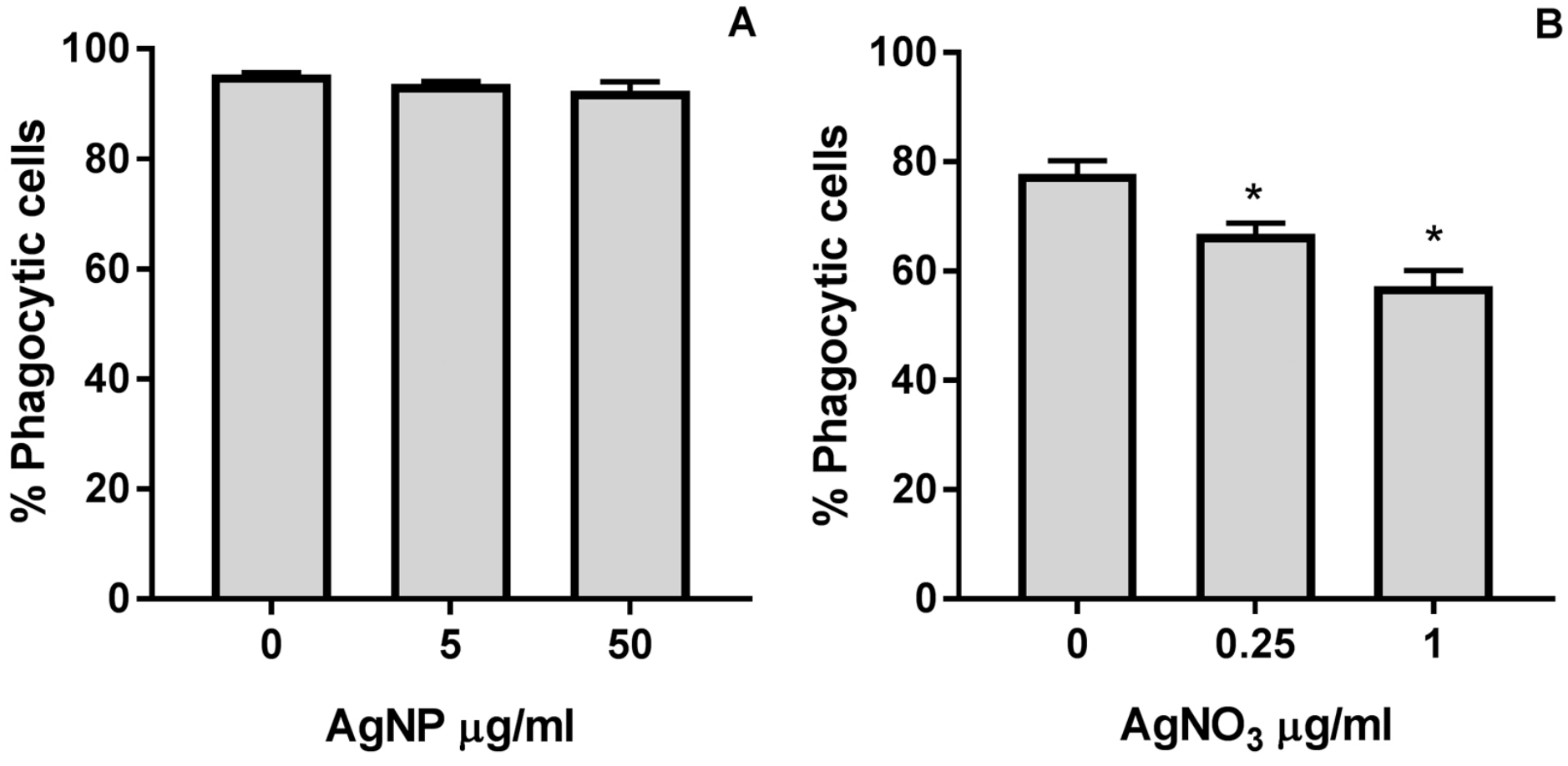
A
100
80
60
40
20
0
% Phagocytic cells
0
5
50
AgNP μg/ml
B
100
80
60
40
20
0
% Phagocytic cells
*
*
0
0.25
1
AgNO3 μg/ml

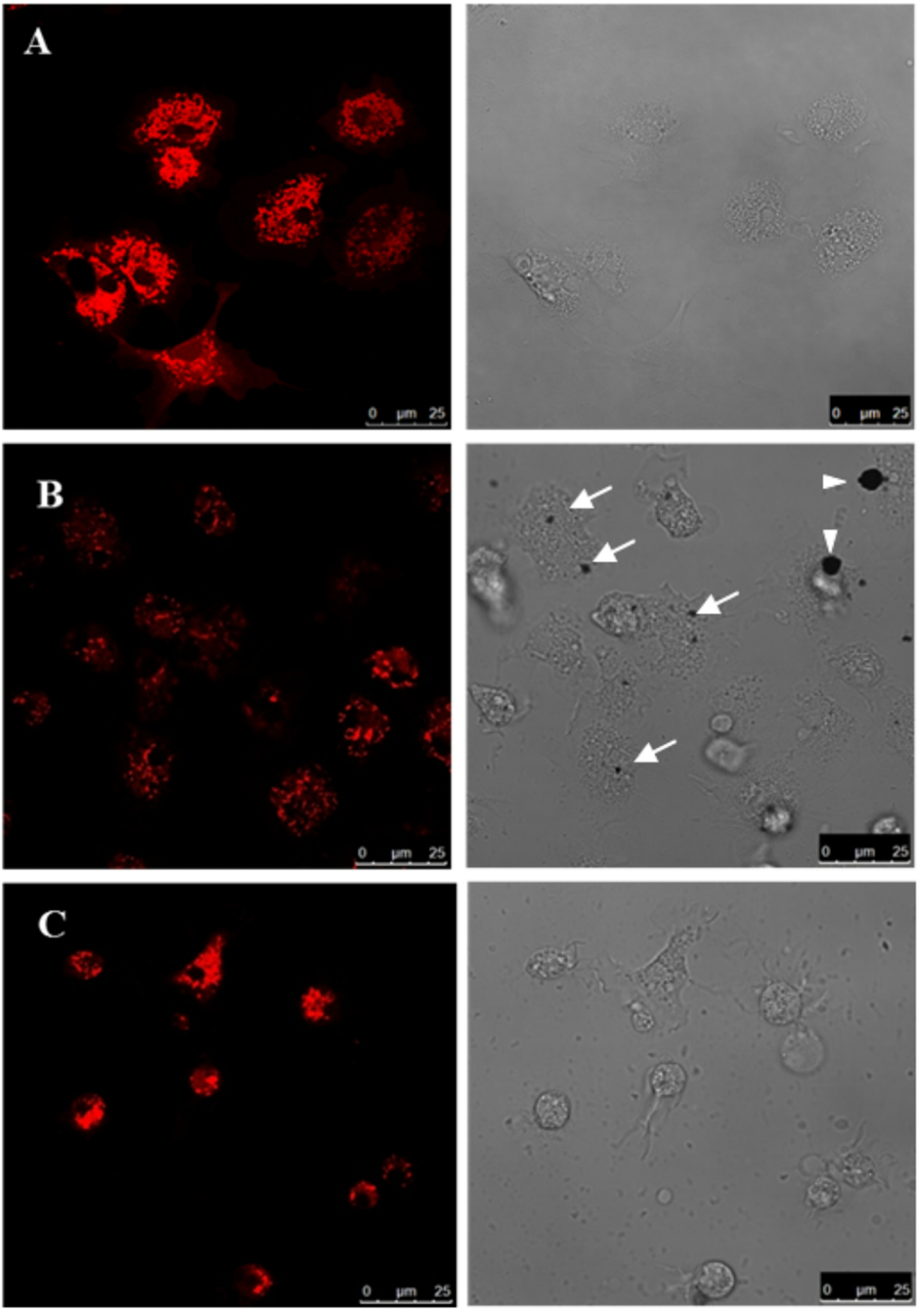
A
0 µm 25
0 µm 25
B
0 µm 25
0 µm 25
C
0 µm 25
0 µm 25

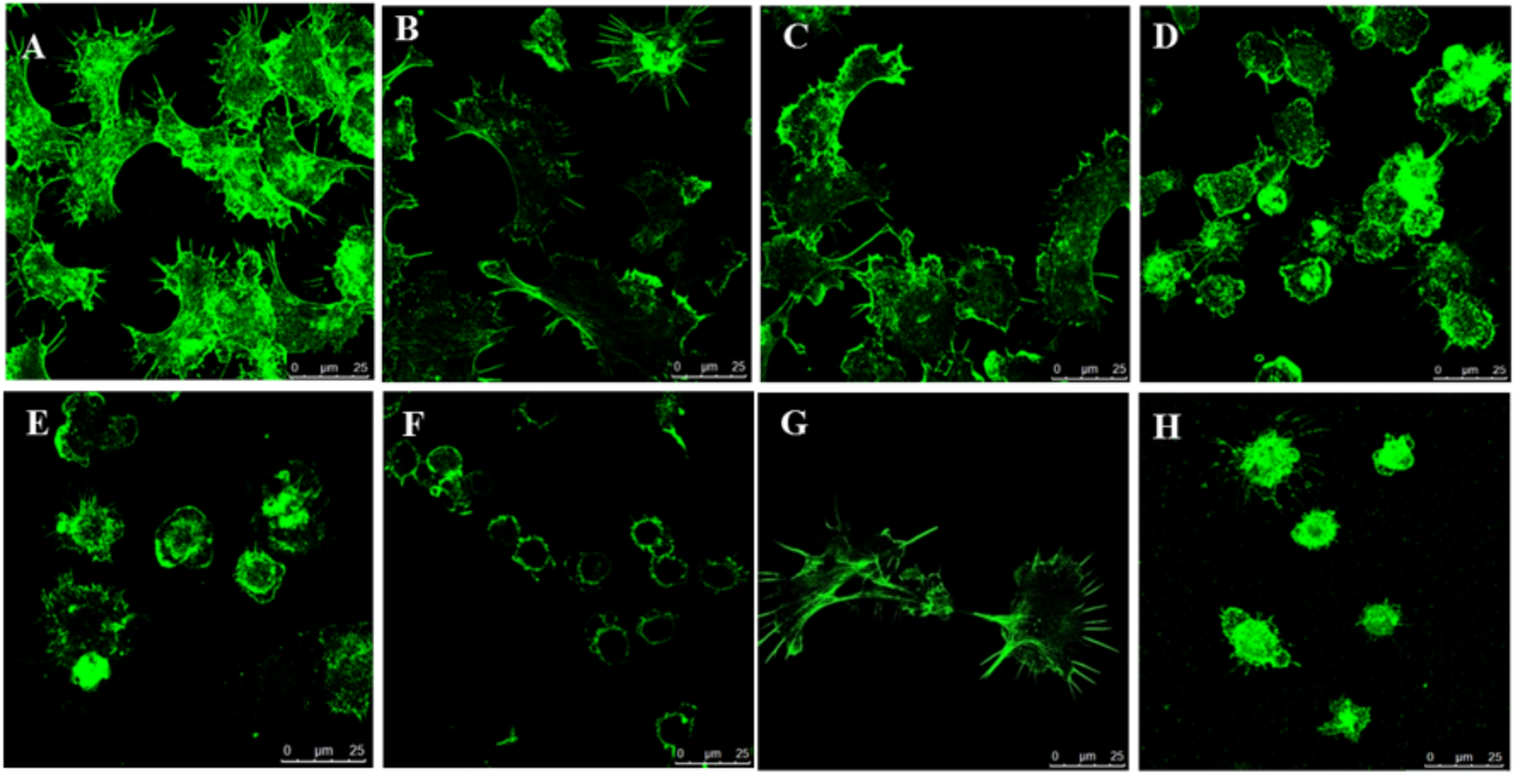
A
B
C
D
E
F
G
H
0 µm 25

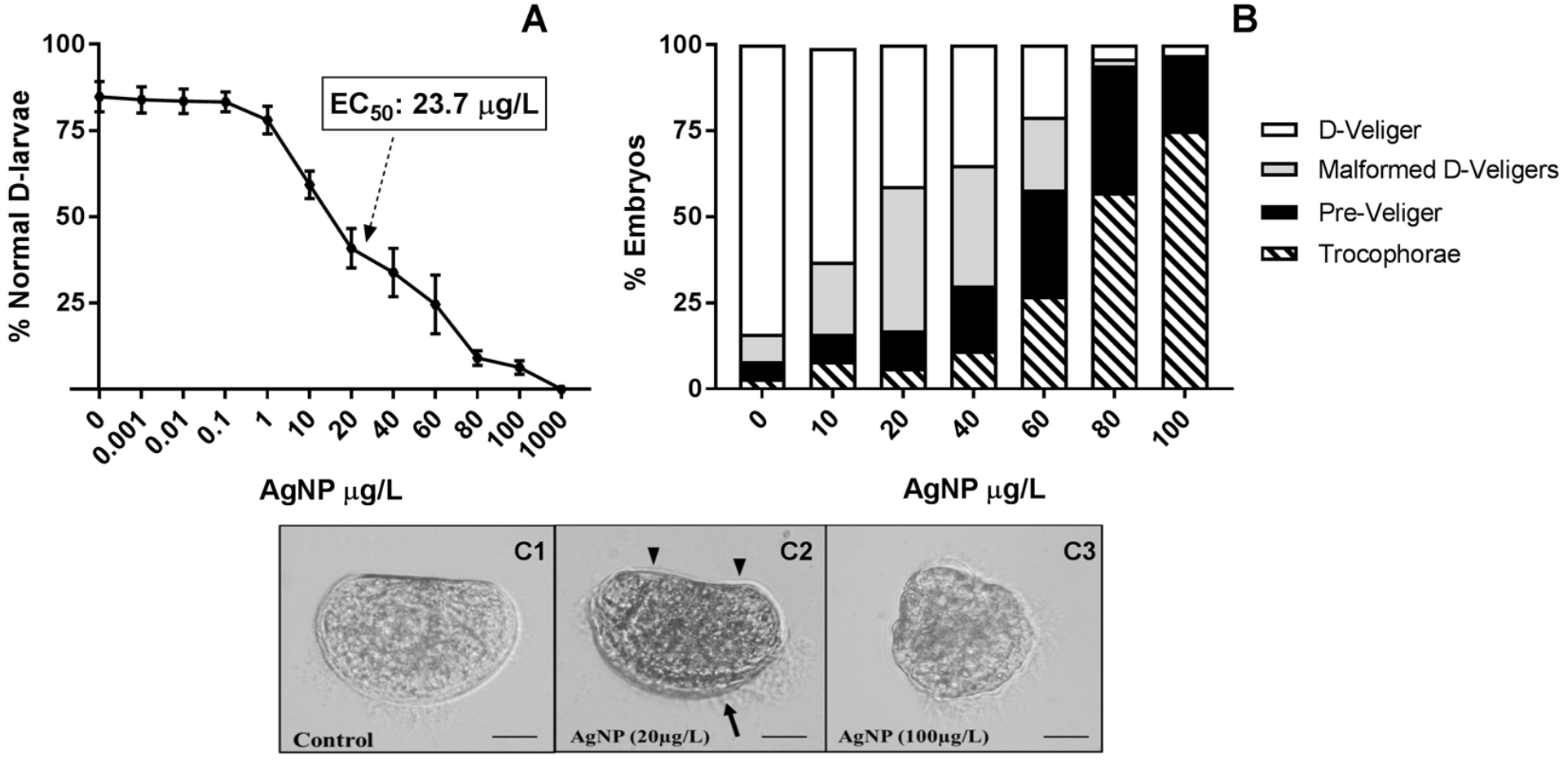
A
100
75
50
25
% Normal D-larvae
EC50: 23.7 µg/L
0
0.001
0.01
0.1
1
10
20
40
60
80
100
1000
AgNP µg/L
B
100
75
50
25
0
% Embryos
0
10
20
40
60
80
100
AgNP µg/L
D-Veliger
Malformed D-Veligers
Pre-Veliger
Trocophorae
C1
Control
C2
AgNP (20µg/L)
C3
AgNP (100µg/L)

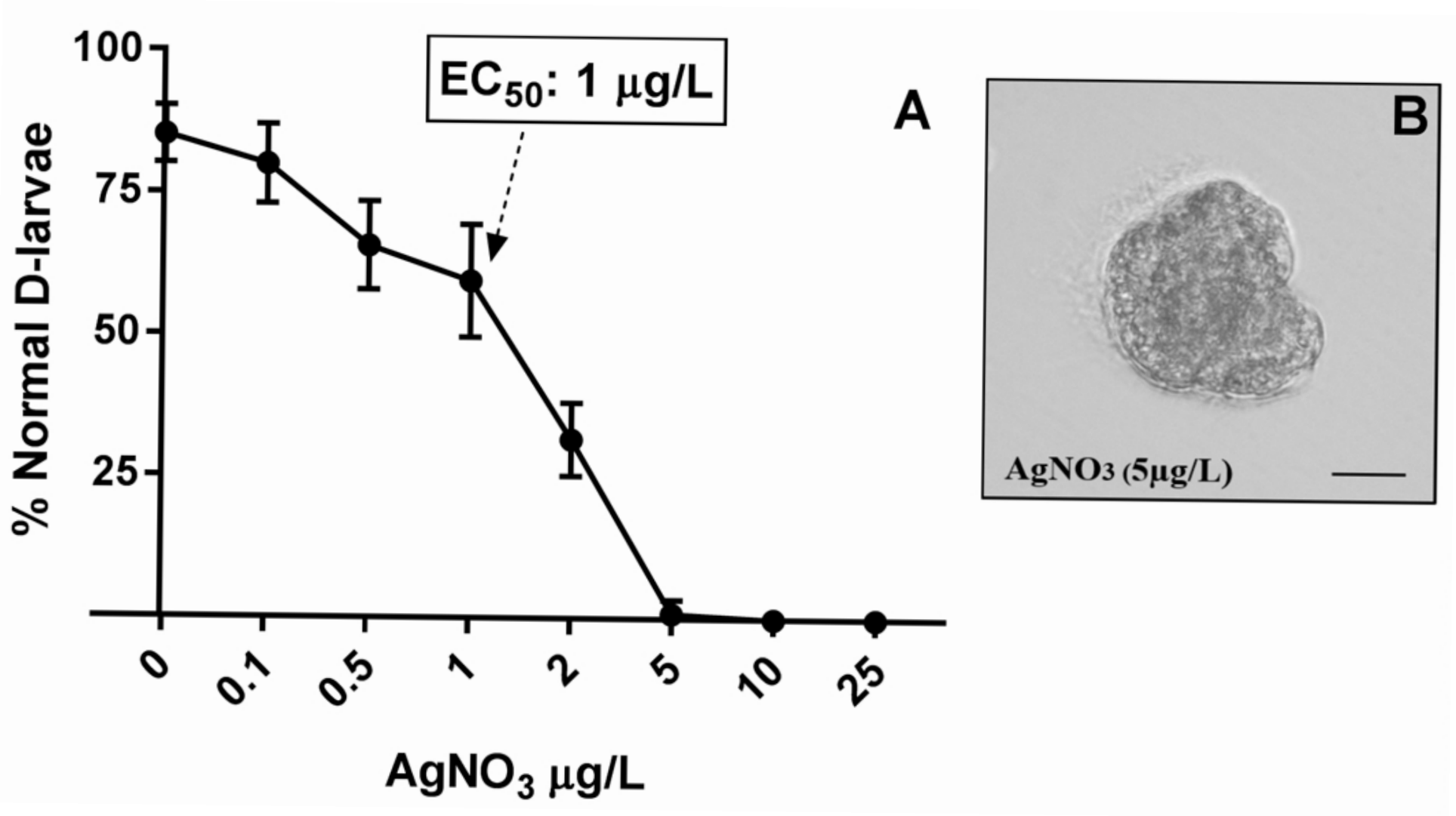
100
75
50
25
% Normal D-larvae
EC50: 1 µg/L
A
B
AgNO3 (5µg/L)
0
0.1
0.5
1
2
5
10
25
AgNO3 µg/L